Arylonium Photoacid Generators Containing Environmentally Compatible Aryloxyperfluoroalkanesulfonate Groups

Ramakrishnan Ayothi,† Yi Yi,† Heidi B. Cao,‡ Wang Yueh,‡ Steve Putna,‡ and Christopher K. Ober*,†

Department of Materials Science and Engineering, Cornell University, Ithaca, New York 14853, and Intel Corporation, Hillsboro, Oregon 97124

Received November 23, 2006. Revised Manuscript Received January 10, 2007

Photoacid generators (PAGs) producing environmentally benign 2-phenoxytetrafluoroethanesulfonate fluoroorganic sulfonic acids were synthesized. Synthesis and characterization of the new PAGs composed of 2-phenoxytetrafluoroethanesulfonate with diphenyliodonium or triphenylsulfonium units are described. Characteristics of the onium PAGs were evaluated and compared with perfluorobutanesulfonate (PFBS)-based onium PAGs. The newly synthesized compounds efficiently produced sulfonic acid photochemically upon exposure to selected radiation (254 nm, e-beam, and 13.4 nm wavelengths). The sulfonic acid generated from the new PAGs contains far fewer perfluorinated carbon atoms than those found in widely used perfluorooctanesulfonate (PFOS) PAGs and successfully catalyzed deprotection of the acid-labile *tert*-butoxycarbonyl, methyladamantyl ester, and *tert*-butyl ester groups present in model positive tone chemically amplified resists (CARs). Their influence on the lithographic performance of chemically amplified resists was investigated using e-beam and extreme ultraviolet (EUV or 13.4 nm) radiation. For the first time, the capability of PFOS-free PAGs for EUV lithographic application in a CAR was demonstrated by comparing resist sensitivity, resolution, and line-edge roughness (LER) with resist formulations containing PFBS-based diphenyliodonium and triphenylsulfonium PAGs. These new PAGs are attractive for lithographic applications as alternatives to the widely used PFOS PAGs because environmental and performance issues require the availability of strong acid PFOS-free photoacid generators.

1. Introduction

Photoacid generators (PAG) are key materials in the curing and imaging processes of photosensitive polymeric materials.[1−3] One of the most important uses of photoacid generators is found in chemically amplified photoresists for microlithography applications.[1,4] Among the most widely used photoacid generating compounds are those that incorporate perfluoroalkanesulfonate (PFAS) groups.[4,5] Their use in photoacid generators not only produces strong acid but also offers several advantages, including superior physicochemical properties, excellent lithographic performance, and process compatibility.[4,5] However, the recent finding that perfluoroalkanesulfonate (PFAS) compounds with more than four consecutive CF_2 units are environmental hazards[6,7] requires the creation of alternative materials with similar outstanding characteristics. This paper describes one approach to new environmentally friendly photoacid generators.

Identifying new PFAS-free photoacid generators is important, because chemically amplified resist (CAR) materials using photoacid catalysis are the cornerstone of DUV lithography and because they offer very valuable benefits to the patterning process, of which high radiation sensitivity and enhanced resolution are the two most striking examples.[4,8,9] The continuous reduction in exposure wavelength (365 to 193 nm) along with ongoing improvements of CAR materials during the last few decades have been among the most important factors enabling the miniaturization of memory and microprocessor chips.[4,10] Chemically amplified photoresists are now being implemented to produce 90 nm microelectronic circuit patterns and will be used in the development of 65 nm and smaller microelectronic devices.[4] Imaging systems based on 193 nm immersion[11,12] and EUV radiation[13,14] are under vigorous development for the fabrication of sub-50 nm features. In recent years, EUV patterning has emerged as a promising next generation lithography

* Corresponding author. Phone: (607) 255 -8417. Fax: (607) 255-2365. E-mail: cober@ccmr.cornell.edu.
† Cornell University.
‡ Intel Corporation.

(1) Fréchet, J. M. J. *Pure Appl. Chem.* **1992**, *64*, 1239.
(2) Shirai, M.; Tsunooka, M. *Bull. Chem. Soc. Jpn.* **1998**, *71*, 2483.
(3) Crivello, J. V. *J. Polym. Sci., Part A: Polym. Chem.* **1999**, *37*, 4241.
(4) Ito, H. *Adv. Polym. Sci.* **2005**, *172*, 37.
(5) Suzuki, Y.; Johnson, D. W. *Proc. SPIE* **1998**, *3333*, 735.
(6) Kannan, K.; Koistinen, J.; Beckmen, K.; Evans, T.; Gorzelany, J. F.; Hansen, K. J.; Jones, O. P. D.; Helle, E.; Nyman, M.; Giesy, J. P. *Environ. Sci. Technol.* **2001**, *35*, 1593.
(7) Martin, J. W.; Mabury, S. A.; Solomon, K. R.; Muir, D. C. G. *Environ. Toxicol. Chem.* **2003**, *22*, 196.
(8) Reichmanis, E.; Houlihan, F. M.; Nalamasu, O.; Neenan, T. X. *Chem. Mater.* **1991**, *3*, 394.
(9) Wallraff, G. M.; Hinsberg, W. D. *Chem. Rev.* **1999**, *99*, 1801.
(10) Brunner, T. A. *J. Vac. Sci. Technol., B* **2003**, *21*, 2632.
(11) Dammel, R.; Houlihan, F. M.; Sakamuri, R.; Rentkiewicz, D.; Romano, A. *J. Photopolym. Sci. Technol.* **2004**, *17*, 587.
(12) Rothschild, M.; Bloomstein, T. M.; Kunz, R. R.; Liberman, V.; Switkes, M.; Palmacci, S. T.; Sedlacek, J. H. C.; Hardy, D.; Grenville, A. *J. Vac. Sci. Technol., B* **2004**, *22*, 2877.
(13) Service, R. F. *Science* **2001**, *293*, 785.
(14) Wang, Y.; Cao, H. B.; Chandhok, M.; Lee, S.; Shumway, M.; Bokor, J. *Proc. SPIE* **2004**, *5376*, 434.

10.1021/cm062802k CCC: $37.00 © 2007 American Chemical Society
Published on Web 02/22/2007

(NGL) technique for the production of 32 nm features.[13−19] Feature sizes as small as 30 nm have already been demonstrated using CAR, thereby suggesting that these strategies will continue to play a crucial role for the development of 193 nm immersion[11,20,21] and EUV lithography.[14−18,22,23]

Chemically amplified resists are highly tuned mixtures of several components.[4] A photoacid generator (PAG) is one of the critical components used in a CAR regardless of the DUV exposure wavelength that produces acid upon irradiation.[1−4] The generated photoacid catalyzes important chemical transformations within the film, generally referred to as chemical amplification (CA), such as deprotection, polymerization initiation, chain scission, or cross-linking under mild thermal conditions.[4] The presence of a PAG in the chemically amplified resist amplifies the weak radiation signal to a strong chemical signal and thereby offers flexibility to resist design by providing the spatial resolution and sensitivity required in the production of high-density integrated circuit components.[9,10] Many ionic and nonionic photoacid-generating compounds have been developed and investigated for microlithography applications.[1,2,24−26] Ionic PAGs are preferentially used in all the advanced CAR formulations because of their excellent quantum yields of acid generation and high thermal and formulation stability.[3−5,27−30]

The most widely used ionic PAGs in chemically amplified resists are onium salts, which contain a photosensitive iodonium or sulfonium cation and a negatively charged non-nucleophilic counterion.[4] The mechanism of photoacid generation of onium PAGs has been studied in detail and is well-documented in the literature.[3,27,31,32] The nature of the photoacid produced upon irradiation of the PAG is directly related to the anion of the ionic PAG. Differences in the acid strength, boiling point, size, miscibility, and stability of the photoacid produced directly influence a variety of parameters related to photoresist performance, including sensitivity, resolution, and image profiles.[33−35] Several non-nucleophilic anions, including fluorinated inorganic anions, organic sulfonates, and PFAS such as $CF_3SO_3^-$ (triflate), $C_4F_9SO_3^-$ (PFBS), and $C_8F_{17}SO_3^-$ (PFOS), have been considered for lithographic applications.[4] However, PFBS and PFOS are the two anions that most satisfy the lithographic process and its performance-related factors.[4,5,36] PFOS-based PAGs became the primary choice for CAR systems because they have numerous advantages, including high quantum yield for acid generation, excellent resist miscibility, good thermal and storage stability in resist films, and suitable diffusion length.[4,5] However, recent investigations of the bioaccumulation and toxic nature of PFAS compounds containing four or more CF_2 units indicate these compounds may no longer be environmentally acceptable in CAR processes.[6,7,37−39] In addition to environmental concerns, there are performance issues involving the use of PFOS in emerging lithographic resists that include undesirable self-assembly,[40] leaching in immersion media,[20] and absorption of EUV radiation.[41,42] The PFOS issue has left PFBS as the only currently viable anion for CAR. The use of PFBS is limited because of its persistent nature,[43] and it has been proposed by several organizations that it is also in need of replacement.[44]

The design of environmentally compatible PFOS-free PAG anions that satisfies NGL requirements without additional complexity is a significant challenge. The approaches currently described for the elimination of PFOS from PAGs can be grouped into two categories. In the first category, various fluorinated sulfonates or functionalized fluorinated sulfonates were designed that have fewer perfluorinated carbon atoms than found in PFOS.[45,46] In the second category, fluorinated

(15) Kinoshita, H.; Watanabe, T. *J. Photopolym. Sci. Technol.* **2000**, *13*, 379.
(16) Cao, H. B.; Wang, Y.; Rice, B. J.; Roberts, J.; Bacuita, T.; Chandhok, M. *Proc. SPIE* **2004**, *5376*, 757.
(17) Oizumi, H.; Tanaka, Y.; Shiono, D.; Hirayama, T.; Hada, H.; Onodera, J.; Yamaguchi, A.; Nishiyama, I. *J. Photopolym. Sci. Technol.* **2006**, *19*, 507.
(18) Thackeray, J. W.; Nassar, R. A.; Spear-Alfonso, K.; Wallow, T.; LaFontaine, B. *J. Photopolym. Sci. Technol.* **2006**, *19*, 525.
(19) Bratton, D.; Yang, D.; Dai, J.; Ober, C. K. *Polym. Adv. Technol.* **2006**, *17*, 94.
(20) Hinsberg, W.; Wallraff, G. M.; Larson, C. E.; Davis, B. W.; Deline, V.; Raoux, S.; Miller, D.; Houle, F. A.; Hoffnagle, J.; Sanchez, M. I.; Rettner, C.; Sundberg, L. K.; Medeiros, D. R.; Dammel, R. R.; Conley, W. E. *Proc. SPIE* **2004**, *5376*, 21.
(21) Taylor, J. C.; LeSuer, R. J.; Chambers, C. R.; Fan, F.-R. F.; Bard, A. J.; Conley, W. E.; Willson, C. G. *Chem. Mater.* **2005**, *17*, 4194.
(22) Wallraff, G. M.; Medeiros, D. R.; Sanchez, M.; Petrillo, K.; Huang, W. S.; Rettner, C.; Davis, B.; Larson, C. E.; Sundberg, L.; Brock, P. J.; Hinsberg, W. D.; Houle, F. A.; Hoffnagle, J. A.; Goldfarb, D.; Temple, K.; Wind, S.; Bucchignano, J. *J. Vac. Sci. Technol., B* **2004**, *22*, 3479.
(23) Dai, J.; Chang, S. W.; Hamad, A.; Yang, D.; Felix, N.; Ober, C. K. *Chem. Mater.* **2006**, *18*, 3404.
(24) Houlihan, F. M.; Neenan, T. X.; Reichmanis, E.; Kometani, J. M.; Chin, T. *Chem. Mater.* **1991**, *3*, 462.
(25) Hanson, J. E.; Reichmanis, E.; Houlihan, F. M.; Neenan, T. X. *Chem. Mater.* **1992**, *4*, 837.
(26) Neenan, T. X.; Houlihan, F. M.; Reichmanis, E.; Kometani, J. M.; Bachman, B. J.; Thompson, L. F. *Macromolecules* **1990**, *23*, 145.
(27) Pappas, S. P. *J. Imaging Technol.* **1985**, *11*, 146.
(28) Kozawa, T.; Yoshida, Y.; Uesaka, M.; Tagawa, S. *Jpn. J. Appl. Phys.* **1992**, *31*, 4301.
(29) Yamamoto, H.; Kozawa, T.; Nakano, A.; Okamoto, K.; Tagawa, S.; Ando, T.; Sato, M.; Komano, H. *J. Vac. Sci. Technol., B* **2005**, *23*, 2728.
(30) Nakano, A.; Kozawa, T.; Tagawa, S.; Szreder, T.; Wishart, J. F.; Kai, T.; Shimokawa, T. *Jpn. J. Appl. Phys. Lett.* **2006**, *45*, L194−L196.
(31) Dektar, J. L.; Hacker, N. P. *J. Org. Chem.* **1990**, *55*, 639−47.
(32) Dektar, J. L.; Hacker, N. P. *J. Am. Chem. Soc.* **1990**, *112*, 6004−15.
(33) Allen, R. D.; Opitz, J.; Larson, C. E.; DiPietro, R. A.; Breyta, G.; Hofer, D. C. *Proc. SPIE* **1997**, *3049*, 44.
(34) Ablaza, S. L.; Cameron, J. F.; Xu, G.; Yueh, W. *J. Vac. Sci. Technol., B* **2000**, *18*, 2543.
(35) Croffie, E.; Yuan, L.; Cheng, M.; Neureuther, A.; Houlihan, F.; Cirelli, R.; Watson, P.; Nalamasu, O.;Gabor, A. *J. Vac. Sci. Technol., B* **2000**, *18*, 3340.
(36) Pohlers, G.; Barclay, G. G.; Razvi, A.; Stafford, C.; Barbieri, A.; Cameron, J. F. *Proc. SPIE* **2004**, *5376*, 79.
(37) Giesy, J. P.; Kannan, K. *Environ. Sci. Technol.* **2001**, *35*, 1339.
(38) Bowden, M. J.; Beu, L.; Pawsat, S. *Proc. Electrochem. Soc.* **2002**, *2002−15*, 200.
(39) Kannan, K.; Corsolini, S.; Falandysz, J.; Fillmann, G.; Kumar, Kurunthachalam, S.; Loganathan Bommanna, G.; Mohd Mustafa, A.; Olivero, J.; Van Wouwe, N.; Yang Jae, H.; Aldoust Kenneth, M. *Environ. Sci. Technol.* **2004**, *38*, 4489.
(40) Lenhart, J. L.; Fischer, D. A.; Sambasivan, S.; Lin, E. K.; Jones, R. L.; Soles, C. L.; Wu, W.-l.; Goldfarb, D. L.; Angelopoulos, M. *Langmuir* **2005**, *21*, 4007.
(41) Szmanda, C. R.; Brainard, R. L.; Mackevich, J. F.; Awaji, A.; Tanaka, T.; Yamada, Y.; Bohland, J.; Tedesco, S.; Dal'Zotto, B.; Bruenger, W.; Torkler, M.; Fallmann, W.; Loeschner, H.; Kaesmaier, R.; Nealey, P. M.; Pawloski, A. R. *J. Vac. Sci. Technol., B* **1999**, *17*, 3356.
(42) Kwark, Y.-J.; Bravo-Vasquez, J. P.; Chandhok, M.; Cao, H.; Deng, H.; Gullikson, E.; Ober, C. K. *J. Vac. Sci. Technol., B* **2006**, *24*, 1822.
(43) PFBS technical data bulletin is available on the internet at http://cms.3m.com/cms/us/en/2−56./ccuikFO/vieimage.jhtml.
(44) World Semiconductor Council agreement on PFOS is available on the internet at http://www.sia-online.org/downloads/2006_PFOS_agreement.pdf.

nitrogen, carbon-centered anions,[47] and carborane[48] compounds have been proposed. Regrettably, the current literature provides few reliable guidelines for identifying new PFOS-free photoacid generator anions. Key considerations in the design of a novel PFOS-free PAG anion that include both performance and environmentally related features remain unexplored. Furthermore, very little is known about the lithographic performance of PFOS-free PAG in next-generation lithographies such as EUV-based patterning.To understand such materials and address both environmental and performance issues, we have designed selected ionic PAGs carrying a PFOS-free photoacid precursor that are based on fluoroalkanesulfonic acids containing a short perfluorinated group ($CF_2 < 4$).[49] In this paper, we first describe the strategy used to design a PFOS-free anion with special emphasis on EUV lithography. We then report the preparation, characterization, and properties of diphenyliodonium (DPI) and triphenylsulfonium (TPS) PAGs containing the 2-phenoxytetrafluoroethanesulfonate group. Finally, we demonstrate the capabilities of the new PAGs by comparing the performance for resist compositions containing new PAGs with those of standard PFBS PAGs patterned using e-beam and EUV radiation.

2. Experimental Section

2.1. Materials. Phenol (product number (P No.) 185450, ≥99%), potassium hydroxide solution (KOH, 1.0 N in methanol, P No. 319384), sodium dithionite ($Na_2S_2O_4$, P No. 13351, >86%), sodium tungstate dihydrate ($Na_2WO_4 \cdot 2H_2O$, P No. 223336, 99%), diphenyliodonium chloride (P No. D209082, 97%), copper(II) acetate (P No. 517453, 99.999%), diphenyl sulfide (P No. P35316, 98%), dimethyl sulfoxide (DMSO, P No. 276855, anhydrous, ≥99.9%), acetonitrile (P No. 360457, ACS reagent, ≥99.5%) propylene glycol monomethyl ether acetate (PGMEA, P No. 537543, 99%), 2-butanone (P No. 360473, ≥99%), di(propylene glycol) methyl ether (DPGM, P No. 484253, ≥99.9%), propylene glycol methyl ether (PGME, P No.484407, ≥99.5%), ethyl lactate (EL, P No. E34102, 98%), 4-butyrolactone (GBL, P No. B103608, ≥99%), trioctylamine (TOA, P No. T81000, 98%), triphenylsulfonium perfluorobutanesulfonate (TPS PFBS, P No. 531057, ≥99%), and poly(4-hydroxystyrene) (PHS, $M_w = 20\,000$; P No. 436224) were purchased from Sigma-Aldrich and used without further purification. Sodium phosphate (HNa_2O_4P, P No. 71629, ≥99%, Fluka), sodium bicarbonate ($NaHCO_3$, P No. S2333, ACS certified, Fisher), hydrogen peroxide (30% V/V, P No. V34004, Mallinckrodt), and 1,2-dibromotetrafluoroethane (P No. 1100A06, 99%, SynQuest Labs) were used as received. Diphenyliodonium perfluorobutanesulfonate (DPI PFBS) was provided by JSR Corporation. Poly(4-*tert*-butoxycarbonyloxystyrene) ($M_n = 120$ K; $M_w/M_n = 2.1$) was synthesized by free-radical polymerization using AIBN as initiator. Poly(4-hydroxystyrene-*co*-4-*tert*-butoxycarbonyloxystyrene) was synthesized from PHS (Aldrich) using the protecting group chemistry described in the literature.[50] Poly(4-hydroxystyrene-*co*-styrene-*co*-*t*-butyl acrylate) (P(HS-*co*-S-co-tBA); 10% tBA) provided by Maruzen was used for DUV experiments. P(HS-*co*-S-co-*t*BA) (25% tBA) purchased from DuPont was used for DUV and e-beam experiments. Poly(γ-butyrolactone methacrylate-*co*-methyladamantyl methacrylate) (P(GBLMA-*co*-MAdMA); 0.565:0.435) provided by Mitsubishi Rayon was used in both e-beam and EUV evaluation. All other chemicals were obtained from commercial sources and used without further purification. Silicon wafers were purchased from Montco Silicon Technologies, Inc.

2.2. Methods. ^1H (299.763 MHz) and ^{19}F (282.028 MHz) nuclear magnetic resonance (NMR) spectra were recorded on a Varian Mercury 300 spectrometer. The chemical shifts (δ) were reported in parts per million (ppm) relative to corresponding deuterated solvents for ^1H NMR and to CF_3COOH for ^{19}F NMR. GC/MS spectra were obtained with a Hewlett-Packard 5980 gas chromatograph interfaced with a Hewlett-Packard 5970 mass spectrometer that was operated in electron impact (EI) mode. Mass spectra of PAGs were recorded by using an Esquire electrospray ionization (ESI)-based 3D ion trap (Bruker) system available at the Cornell Biotechnology Center. Elemental analysis was performed at the Cornell Nutrient Analysis Lab. UV−VIS measurements were performed by using a Perkin-Elmer λ 10 UV−VIS spectrophotometer. Molar absorption coefficient (ϵ) at 248 nm ($\epsilon_{248\ nm}$) was measured at different concentrations (C), and ϵ_{248} was determined from the slope of the straight line fitted using $A_{248\ nm} = \epsilon C$. FT−IR measurements were performed on a Mattson Instruments Galaxy 2000 series FT−IR. Quartz and double-side-polished silicon substrates were used for UV−VIS and FT−IR thin film experiments. The final transmission spectra of the films were obtained by dividing the transmission spectra of the film by the transmission of the uncoated quartz substrates.[51]

Thermal analysis was performed on a TA instruments Q1000 differential scanning calorimeter (DSC) and a Q500 thermal gravimetric analyzer (TGA) under a nitrogen atmosphere at a heating rate of 10 °C per minute. TGA was used to determine the decomposition temperature (T_d, at 5% weight loss), and DSC was used to measure the melting point (T_m). The film thickness was measured using a Tencor P10 profilometer. The film thickness for both resists coated on silicon wafers and quartz was in the range of 110 ± 10 nm to 130 ± 10 nm. An UVEXS UV spot curing system SCU 110B operating between 250 and 750 nm was used for simple flood-exposure experiments.

EUV absorbance was calculated using the Centre for X-ray Optics (CXRO) interface developed at Lawrence Berkeley National Laboratory (LBNL). A film thickness of 125 nm and PHS bulk density of 1.16 g/cm^3 were used for the calculations.[42] The size of the sulfonic acid in terms of molar volume was estimated by using the ACD alchemy estimation program. The sulfonic acid strength (pKa) was calculated using Taft additive constants.[52] Outgassing experiments were performed at the University of Wisconsin. The detailed procedures of the experiments and quantification methods are available in the literature.[53] DUV (254 nm) lithographic evaluations were performed using Hybrid Technology Group's (HTG) III-HR contact/proximity mask aligner. The lamp power output measured at 254 nm was used to calculate the dose. E-beam lithography was conducted by using a 100 kV Lecia VB6 exposure

(45) Ferreira, L.; Blakeney, A. J.; Spaziano, G. D.; Dimov, O.; Kocab, T. J.; Hatfield, J. P. WO Patent 2002082185.
(46) Lamanna, W. M. U. S. Patent 2004234888.
(47) Lamanna, W. M.; Kessel, C. R.; Savu, P. M.; Cheburkov, Y.; Brinduse, S.; Kestner, T. A.; Lillquist, G. J.; Parent, M. J.; Moorhouse, K. S.; Zhang, Y.; Birznieks, G.; Kruger, T.; Pallazzotto, M. C. *Proc. SPIE* **2002**, *4690*, 817.
(48) Meagley, R. P. U. S. Patent Appl. 2005221220.
(49) Ober, C. K.; Ayothi, R.; Kim, K.-M.; Liu, X.-Q. U. S. Patent Appl. 2005208420.
(50) Chang, S. W.; Ayothi, R.; Bratton, D.; Yang, D.; Felix, N.; Cao, H. B.; Deng, H.; Ober, C. K. *J. Mater. Chem.* **2006**, *16*, 1470.
(51) Crawford, M. K. F. W. B.; Feiring, A. E.; Feldman, J.; French, R. H.; Leffew, K. W.; Petrov, V. A.; Qiu, W.; Schadt, F. L., III; Tran, H. V.; Wheland, R. C.; Zumsteg, F. C. *Proc. SPIE* **2003**, *5039*, 80.
(52) Perrin, D. D.; Dempsey, B.; Serjeant, E. P. *pKa Prediction for Organic Acids and Bases*; Chapman and Hall: London, 1981.
(53) Wang, Y.; Cao, H. B.; Thirumala, V.; Choi, H. *Proc. SPIE* **2005**, *5753*, 765.

Scheme 1. Preparation of 2-Phenoxytetrafluoroethanesulfonate and Its Onium PAGs

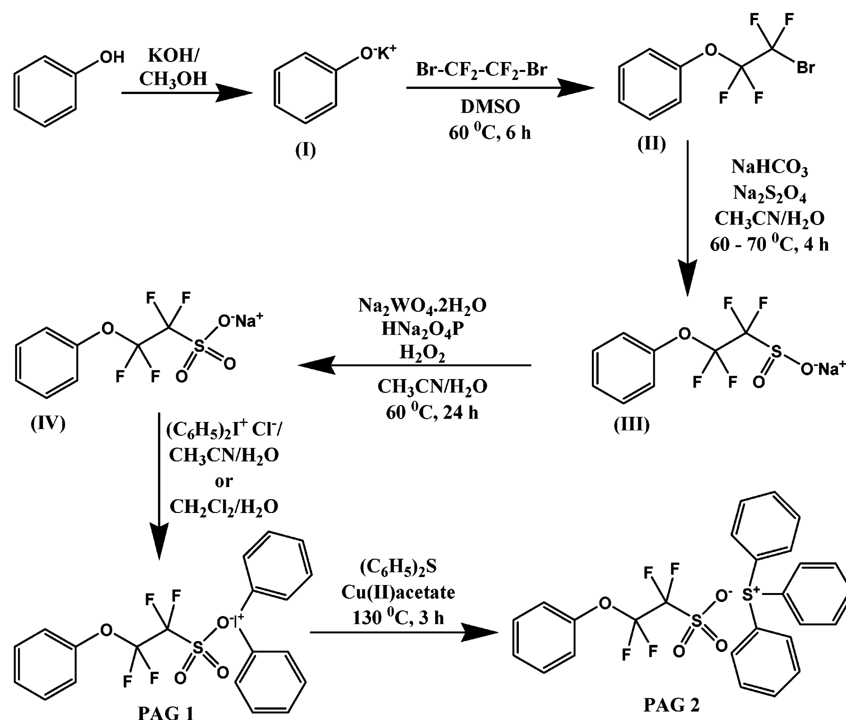

tool at the Cornell Nanoscale Science and Technology Facility (CNF). EUV (13.4 nm) lithography was performed at the Advanced Light Source, LBNL, Berkeley, California. The patterned wafers were examined by using a high-resolution Zeiss scanning electron microscope (SEM). Line-edge roughness (LER) was calculated using SuMMIT image analysis software, EUV technology, Martinez, CA.

2.3. Synthesis and Characterization of PAGs. The synthetic scheme used for the preparation of PAG 1 and 2 is illustrated in Scheme 1.

Potassium Phenoxide (I). Phenol (7.7112 g) was dissolved in 1.0 N KOH in methanol (80 mL) under nitrogen. After being stirred for 30 min at room temperature, the solvent was removed under reduced pressure using a rotary evaporator. The white solid obtained was dried at 120 °C under a vacuum for 12 h and used as prepared for subsequent reaction. Yield = 10.5 g (∼100%).

1-Bromo-2-phenoxytetrafluoroethane (II). In a 500 mL three-neck flask fitted with a refluxing condenser and a dropping funnel was dissolved potassium phenoxide (7.7112 g, 0.0583 mmol phenol) with anhydrous DMSO (28 mL) under nitrogen. 1,2-Dibromotetrafluoroethane (15.2 g, 0.0583 mmol) was added slowly (over ∼15 min) from a dropping funnel at 40 °C. The occurrence of a reaction between phenoxide and the dibromo compound was visualized through immediate color change. After addition of the dibromo compound, the resulting mixture was heated at 60 °C for 6 h. After 6 h, the reaction mixture was cooled to room temperature and diluted with cold water (three times the volume of DMSO). The aqueous layer was extracted with dichloromethane. The combined organic layer was dried over anhydrous Na_2SO_4 and concentrated on a rotary evaporator. The pure compound was obtained as a colorless liquid by vacuum distillation. Yield = 10 g (65%); ^{1}H NMR ($CDCl_3$/CF_3COOH) δ 7.20−7.25, 7.27−7.32, 7.36−7.42; ^{19}F NMR ($CDCl_3$/CF_3COOH) δ −68.54 (−CF_2Br), −86.40 (−OCF_2); GC/MS (*m*/*z*, EI) = 272 (M), 274 (M + 2).

Sodium 2-Phenoxytetrafluoroethanesulfinate (III). In a 250 mL three-neck flask fitted with a condenser and a dropping funnel was added 1-bromo-2-phenoxytetrafluoroethane (9.5 g, 0.035 mmol) into deoxygenated aqueous acetonitrile solution (110 mL H_2O and 55 mL acetonitrile) containing $NaHCO_3$ (6.46 g, 0.0769 mmol) and $Na_2S_2O_4$ (12.1098 g, 0.069 mmol) under nitrogen at room temperature. The mixture was heated at 60 °C for 1 h and heated for another 3 h at 70 °C. The two-phase solution obtained was cooled to room temperature and ethyl acetate was added. The aqueous solution was extracted with a small amount of ethyl acetate several times. Finally, the ethyl acetate layer was washed with a saturated solution of sodium chloride and dried over anhydrous Na_2SO_4. The waxy solid obtained after removal of ethyl acetate was converted to solid sodium sulfinate by washing with hexane several times. It was further purified by using isopropanol and hexane. Yield = 6.5 g (61%); ^{1}H NMR (D_2O/CF_3COOH) δ 7.29−7.35, 7.42−7.46; ^{19}F NMR (D_2O/CF_3COOH) δ −82.36 (−OCF_2), −132.95 (−CF_2SO_2-Na).

Sodium 2-Phenoxytetrafluoroethanesulfonate (IV). In a 100 mL three-neck flask fitted with a condenser and a dropping funnel was slowly added a hydrogen peroxide solution (∼5 mL) to a stirred aqueous acetonitrile solution (12 mL of H_2O and 20 mL of acetonitrile) of 2-phenoxytetrafluoroethanesulfinate (6 g, 0.021 mmol), sodium tungstate dihydrate (4.21 g, 0.0107 mmol), and sodium hydrogen phosphate (1.521 g, 0.0107 mmol) under nitrogen at room temperature. The complete dissolution of all inorganic salts occurred during the addition of hydrogen peroxide. The progress of the reaction was inferred by the exothermic nature of the reaction and the color change. The mixture was heated at 60 °C for 24 h. After 24 h, the reaction mixture was cooled to room temperature, and the solvents were removed under reduced pressure. The waxy solid obtained was extracted with isopropanol. Pure sodium sulfonate was isolated by removing the solvent and final washing was carried out several times with hexane. Yield = 4.5 g (71%); ^{1}H NMR (D_2O/CF_3COOH) δ 7.31 − 7.38, 7.43 − 7.49; ^{19}F NMR (D_2O/CF_3COOH) δ −82.27 (−OCF_2), −118.13 (−CF_2SO_3Na).

Diphenyliodonium 2-Phenoxytetrafluoroethanesulfonate (PAG 1). Method 1. To a solution of sodium sulfonate (IV, 3.6 g, 0.0122 mmol) in 40 mL of acetonitrile was added diphenyliodonium chloride (3.843 g, 0.0122 mmol). Distilled water (∼15 mL) was added until the diphenyliodonium chloride was completely soluble. The homogeneous solution was heated at 60 °C for 6 h. After the

reaction, the solvents were removed under reduced pressure. Addition of ethyl acetate resulted in precipitation of excess diphenyliodonium chloride and inorganic solids. The solids were removed by filtration. Viscous oil was obtained after removing the solvents under reduced pressure. The viscous oil obtained was washed with ether several times to get a white solid. *Method II.* To a solution of sodium sulfonate (IV, 3.5 g, 0.0118 mmol) in 30 mL of water was added diphenyliodonium chloride (3.74 g, 0.0118 mmol) suspended in 60 mL of dichloromethane. The two-phase reaction mixture was stirred at room temperature for 12 h. After 12 h, the reaction mixture was separated into aqueous and organic phases; the aqueous phase was extracted several times with dichloromethane. The combined extracts were then dried with anhydrous Na_2SO_4 and filtered. Viscous oil was obtained after removing the solvent under reduced pressure. The viscous oil obtained was washed with ether several times to get a white solid. The solid obtained by both methods was purified by dissolving it in either dichloromethane or acetone and precipitating it in ether. Analytically pure PAG was obtained by either repeating the precipitation cycle 3−5 times or recrystallizing it in a CH_2Cl_2/ether mixture. Yield = 3.9 g (60%, method I) and yield = 4.3 g (65%, method II); ^{1}H NMR (acetone-d6) δ 7.23−7.31, 7.38−7.45, 7.54−7.60, 7.69−7.74, 8.28−8.33; ^{19}F NMR (acetone-d6) δ −82.38 (OCF_2), −118.04 ($CF_2SO_3^-$). Elemental anal. Calcd: C, 43.34. Found: C, 43.84. LC-MS (negative mode ESI, *m/z*, %) 273.1 (100%, $C_8H_5F_4O_4S^-$); LC-MS (positive mode ESI, *m/z*, %) 154.5 (19%, $C_{12}H_{10}$), 281.0 (81%, $C_{12}H_{10}I^+$); T_d = 165 °C; T_m = 134 °C; UV (acetonitirle, λ, nm) 275−250 (weak), 250−225 (strong), and 215−200 (very strong); $\epsilon_{248\ nm}$ (acetonitrile, $M^{-1}\ cm^{-1}$) 6015.

Triphenylsulfonium 2-Phenoxytetrafluoroethanesulfonate (PAG 2). To diphenyliodonium 2-phenoxytetrafluoroethanesulfonate (PAG 1, 2.82 g, 0.051 mmol) was added, under nitrogen, diphenyl sulfide (0.9476 g, 0.051 mmol) and copper(II) acetate (0.0225 g, 1.2408 $\times 10^{-4}$ mmol). This mixture was heated to 130 °C for 3 h under nitrogen. The reaction mixture was cooled, and the viscous oil obtained was triturated several times with ether. The solid obtained after washing with ether was dissolved in dichloromethane, and precipitation in ether results in a solid with contamination from copper salt. The copper salt was removed by treating a dilute CH_2Cl_2 solution with neutral alumina. The product obtained after alumina treatment was further purified by either the dissolution and precipitation in CH_2Cl_2/ether 3−5 times or recrystallization in a CH_2Cl_2/ether mixture. Yield = 2 g (71%). ^{1}H NMR (acetone-d6) δ 7.24−7.29 (3H), 7.34−7.43 (2H), 7.82−7.96 (15H); ^{19}F NMR (acetone-d6) δ −82.34 ($-OCF_2$), −118.04 ($-CF_2-SO_3^-$); LC-MS (negative mode ESI, *m/z*, %) 273.1 (100%, $C_8H_5F_4O_4S^-$); LC-MS (positive mode ESI, *m/z*, %) = 154.1 (2%, $C_{12}H_{10}$), 186.1 (4%, $C_{12}H_{10}S$), 263.1 (93%, $C_{18}H_{15}S^+$); Elemental anal. Calcd: C, 58.20. Found: C, 57.54. T_d = 305 °C; T_m = 93 °C; UV (acetonitrile, λ, nm) 275−250 (weak), 250−225 (strong), and 215−200 (very strong); $\epsilon_{248\ nm}$ (acetonitrile, $M^{-1}\ cm^{-1}$) 15887.

2.4. Resist Processing for E-beam and EUV Lithography. The photoresist solutions were prepared by dissolving polymer (0.18 g, 6 wt %) and a PAG (~5 wt % relative polymer) into 2.82 g of PGMEA (for P(HS-*co*-S-co-tBA)) or a PGMEA/2-butanone mixture (0.8:0.2, for P(GBLMA-*co*-MAdMA)). The PAG weight percent incorporated in the resist was adjusted so as to keep the molar concentration the same as that for DPI PFBS. TOA (0.06 wt %) was added to the polymer/PAG mixture. The solutions were stirred until complete dissolution of components was observed. Finally, the solutions were filtered through 0.45 μm PTFE filters (Whatman). Photoresist films were spin-coated (3000 rpm) onto hexamethyldisilazane (HMDS) vapor-primed, oxidized silicon wafers and prebaked at a selected temperature for 60 s. The film thickness was in the range of 110 $\pm$ 10 to 130 $\pm$ 10 nm. Resist-coated wafers were exposed to the appropriate radiation. A lithographic pattern profile ranging from 1 μm to 30 nm for E-beam and 120 to 10 nm for EUV was projected onto the resist film. Areas on the wafer were exposed with 12−40 $\mu C/cm^2$ of e-beam radiation or with 4.9−15 mJ/cm^2 of EUV radiation. The minimum dose used for PAG 2 and TPS PFBS was 6 mJ/cm^2, whereas a minimum dose of 4.9 mJ/cm^2 was used for formulations containing PAG 1 and DPI PFBS. The irradiated films were then baked at a specified temperature for 60 s. The films were developed in aqueous tetramethylammonium hydroxide (0.26 N TMAH; AZ 300 MIF) for 30 s, rinsed in distilled water, and dried with a stream of nitrogen. Pattern formation was qualitatively analyzed using optical microscopy and then finally using high-resolution SEM.

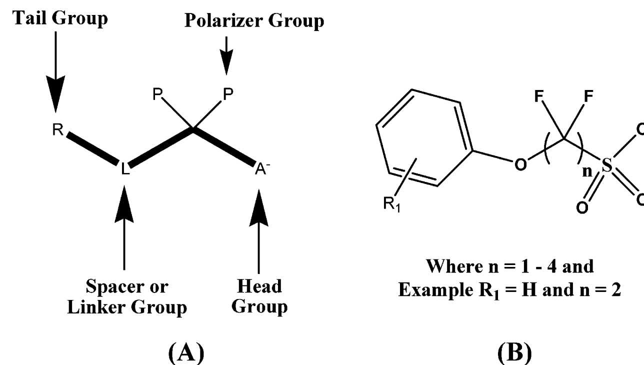

Figure 1. (A) Schematic description of the components present in the PFOS-free PAG anion. (B) Pictorial representation of PFOS-free PAG anion developed for EUVL.

3. Results and Discussion

3.1. Design, Preparation, and Characterization of Photoacid Generators. In exploring alternatives for PFOS anions, we realized that any new PFOS-free PAG anion must possess the attractive characteristics of PFAS but have a reduced fluorine atom or fluoroorganic functional group content to provide both acid generation and environmental acceptance. In addition, the nature of exposing radiation must be considered. On the basis of these requirements, the general structure of PFOS-free photoacid structures designed for both acid generation and environmental concern is depicted in Figure 1A. Knowledge of theoretical (acid size, acid strength, boiling point, absorbance) and experimental (performance) data available on similar compounds was considered.[34,35] In addition, we have also estimated the properties related to the bioaccumulation potential of the compounds along with PFBS and PFOS when we designed the structures. The results are discussed later and the details of the calculation are shown in the Supporting Information. Assessments based on the number of perfluorocarbons and physicochemical properties qualitatively suggest no bioaccumulation for the PFOS-free compounds carrying short perfluorinated groups ($CF_2 \leq 4$). The PFOS-free photoacid structure shown in Figure 1A contains four basic components: (i) the sulfonate group was selected as the acid head group because it is strongly acidic; (ii) a short perfluorinated unit adjacent to the sulfonate group was used to enhance acid strength; (iii) the perfluorinated group was linked to a tail (R) group; and (iv) a small spacer or linker group (L or break-seal) was used to connect the tail and core. The linker group was

incorporated to increase the compatibility of the PAG anion with potential biotic and abiotic processes if exposed to the environment. The tail group may be used to vary acid strength, size, miscibility, and transparency, which is also a function of the exposure wavelength used. The aryloxyperfluoroalkanesulfonate units carrying limited perfluorinated carbon atoms were designed mainly for EUVL applications (Figure 1B). The reduction in perfluorocarbon length along with the presence of an aryl group will increase its transparency at EUV wavelength,[42] whereas at the same time, it is expected to enhance the miscibility with polymeric resists.[54] We decided to focus primarily on aryloxyperfluoroalkanesulfonate anions carrying only two perfluorinated carbon atoms because of their close resemblance with PFBS in terms of performance properties.

The synthetic method used for the preparation of sodium 2-phenoxytetrafluoroethanesulfonate (IV) and the new corresponding onium PAGs (PAG 1 and 2) is depicted in Scheme 1. Compound (IV) was synthesized using a new synthetic approach developed from established procedures.[55−58] Potassium phenoxide was prepared as described in the experimental section. The trace amounts of residual solvents were removed by drying the solid under vacuum at 120 °C. The potassium phenoxide prepared as described above is sufficient for subsequent reaction. In the second step, potassium phenoxide reacted spontaneously with 1,2-dibromotetrafluoroethane with no mercaptan compounds in DMSO at 60 °C. The phenyl ether in the form of a colorless liquid was recovered by vacuum distillation. GC/MS analysis (from the area under the peak) indicated the presence of 80% phenyl ether (II) and 20% hydrogen-terminated product ($C_6H_5-O-CF_2-CF_2-H$). In our hands, we always observed the formation of small amounts of hydrogen-terminated product. However, the side products formed do not interfere with subsequent steps and were removed efficiently by simple hexane washing in the following steps. We confirmed the structure of compound II by using both NMR and GC/MS. Sulfinatodehalogenation of II with sodium dithionite resulted in the corresponding sodium sulfinate (III). The isolation of sodium sulfinate from inorganic impurities was achieved by simple extraction of the reaction mixture with ethyl acetate. The sodium sulfinate (III) was directly converted to sodium sulfonate (IV) using hydrogen peroxide as the oxidizing agent.[58] Generally, the sulfonates are prepared from the corresponding sulfonyl chlorides, which are in turn synthesized from corresponding sodium sulfinates using corrosive chlorinated agents. In contrast to literature reports, we prepared the sodium sulfonate (IV) by a new simple method. The solubility of sulfonate (IV) in polar solvents such as acetonitrile and isopropanol facilitated its isolation in highly pure form.

PAG 1 was synthesized by simple ion-exchange or metathesis reaction (Scheme 1) of photosensitive halide with the sodium sulfonate (IV).[59] The ion-exchange reaction was carried out in either a CH_3CN/H_2O or CH_2Cl_2/H_2O mixture. The PAG was obtained as a pure white solid by both methods as described in the Experimental Section. The triphenylsulfonium PAG 2 was synthesized by copper-assisted arylation of phenyl sulfide with diphenyliodonium PAG.[60] Copper assisted arylation is an attractive method because it allows the synthesis of various symmetric and asymmetric TPS PAGs. The dissolution/precipitation method results in pure PAG similar to conventional recrystallization methods. However, the PAG was always recrystallized using a CH_2Cl_2/ether (or acetone/ether) mixture subsequent to the dissolution/precipitation procedure. In summary, we have successfully isolated new diphenyliodonium 2-phenoxytetrafluoroethanesulfonate (PAG 1) and triphenylsulfonium 2-phenoxytetrafluoroethanesulfonate (PAG 2) in highly pure form as characterized by standard analytical techniques. Proton NMR of PAG 1 and PAG 2 are shown in Figure 2. NMR, GC/MS, and ESI/MS information on both the intermediates and PAGs is provided in the Supporting Information.

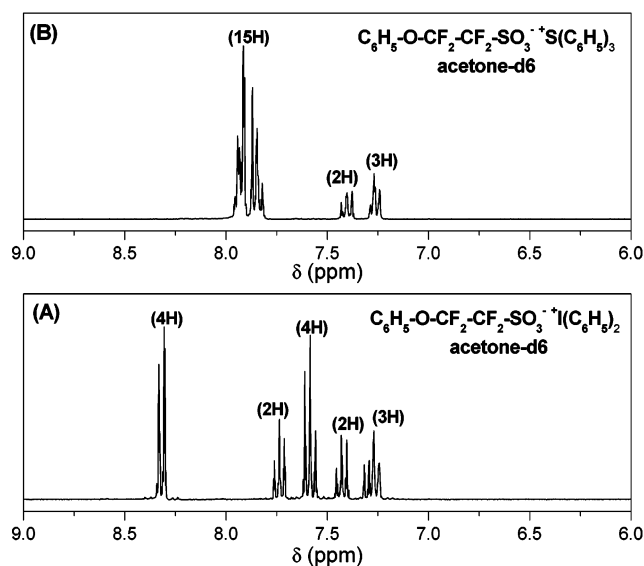

Figure 2. ^{1}H NMR spectra of (A) PAG 1 and (B) PAG 2.

3.2. Physical Characteristics of Photoacid Generators. The use of any PAG in chemical amplification processes requires high solubility in polar solvents, thermal and formulation stability, and most importantly, generation of acid upon exposure to radiation.[4,26,61] In addition, this research was directed at identifying photoacid generators with the potential for superior environmental behavior. Some of the application-related properties determined for PAG 1 and 2 along with standard PAGs are listed in Table 1, whereas the rest of them are discussed in the following section. The illustrations or data corresponding to absorption, photoacid generation, formulation stability, and outgassing characteristics of PAGs are shown in the Supporting Information.

3.2.1. Physicochemical Properties. The new PAGs are readily soluble in common organic solvents (dichlo-

(54) Sundararajan, N.; Keimel, C. F.; Bhargava, N.; Ober, C. K.; Opitz, J.; Allen, R. D.; Barclay, G.; Xu, G. *J. Photopolym. Sci. Technol.* **1999**, *12*, 457.
(55) Rico, I.; Wakselman, C. *J. Fluorine Chem.* **1982**, *20*, 759.
(56) Long, Z.-Y.; Chen, Q.-Y. *J. Org. Chem.* **1999**, *64*, 4775.
(57) Feiring, A. E.; Wonchoba, E. R. *J. Fluorine Chem.* **2000**, *105*, 129.
(58) Mitsui, H.; Zenki, S.; Shiota, T.; Murahashi, S. *J. Chem. Soc., Chem. Commun.* **1984**, 874.
(59) Crivello, J. V.; Lam, J. H. W. *Macromolecules* **1977**, *10*, 1307.
(60) Crivello, J. V.; Lam, J. H. W. *J. Org. Chem.* **1978**, *43*, 3055.
(61) Barclay, G. G.; Medeiros, D. R.; Sinta, R. F. *Chem. Mater.* **1995**, *7*, 1315.

Table 1. Lithographically Relevant Properties of Photoacid Generators

PAG	T_d (°C)	T_m (°C)	$\epsilon_{248\ nm}$ ($M^{-1}\ cm^{-1}$)	resist sensitivity (E_0, mJ/cm^2)
PAG 1	165	134	6015	1.36
DPI PFBS[a]	180	74−84	4200	1.36
PAG 2	305	93	15887	1.53
TPS PFBS[a]	398	84−88	13300	1.70

[a] DPI PFBS and TPS PFBS thermal and absorption properties are shown here for comparison, and the data were taken from reference data published by Sigma-Aldrich.

romethane, ethyl acetate, acetone, and acetonitrile) and polar solvents (PGMEA, DPGM, PGME, EL, GBL, and 2-butanone). In addition to solvents, we also tested PAG miscibility in resist formulations. We prepared both P(HS-*co*-S-*co*-tBA) and P(GBLMA-*co*-MAdMA) photoresist formulations in PGMEA. The PAGs were incorporated at 10 wt % with respect to polymer. The P(HS-*co*-S-*co*-tBA)/PAG resist formulations were prepared immediately before use, whereas P(GBLMA-*co*-MAdMA)/PAG resist combinations including standard PAGs needed 6−7 h of mixing for resist preparation. However, the addition of small amounts of a polar solvent such as 2-butanone enabled the preparation of P(GBLMA-*co*-MAdMA) resists over a few hours. The high solubility of these PAGs in all the preferred solvents as well as in a resist is expected to provide more compositional flexibility and limit the risk of aggregation during storage. The size of the photogenerated acid was estimated in terms of the molar volume using ACD software. The molar volume of the photogenerated acid follows the molecular weight trends within estimated error (±3 cm^3).[34] The acid strength was also estimated using Taft additive constants.[52] The acid strength and size of both $C_6H_5OCF_2CF_2SO_3H$ (pKa = −4.86; size = 170 ± 3 cm^3) and $CF_3CF_2CF_2CF_2SO_3H$ (pKa = −4.99; size = 162 ± 3 cm^3) acids are comparable and the difference is within estimated error. Therefore, similar lithographic performance would be expected if the acid generation efficiency of the PAGs is identical.

3.2.2. Oil−Water Partition Coefficient. In general for a family of compounds, increasing hydrophobicity (lipophilicity) of a compound leads to a greater possibility of bioaccumulation. This behavior is due to the higher octanol−water partition coefficient (P_{OW}) of hydrophobic compounds. The P_{OW} and related properties (biconcentration factor (BCF)) are usually used as a measure of the bioaccumulation traits of a substance. The effect of the number of perfluorinated carbon atoms present in a PFAS compound on the compound's BCF factor and its tendency toward bioaccumulation has been shown in the literature.[7,43] PFBS, which has four perfluorinated carbon atoms, possesses a lower BCF than PFOS and a lower tendency toward bioaccumulation.[7,43] Estimation of P_{OW} and BCF using models accepted by the Environmental Protection Agency shows dramatically lower values for aryloxyperfluoroethanesulfonate compounds than for PFOS (Table 2). This effect may be due to both lower perfluorinated carbon atom content and the presence of additional functional groups. Overall, these results qualitatively suggest low or exceedingly small bioaccumulation for aryloxyperfluoroethanesulfonate compounds. These results make evaluation of the photochemical behavior of these new

Table 2. Environmental Fate of Perfluoroorganic Sulfonic Acids

	properties[a]			
			biodegradation time frame	
sulfonic acid	P_{ow}	BCF	primary	ultimate
$CF_3-CF_2-CF_2-CF_2-SO_3H$	2.4113	3.162	weeks	recalcitrant
$CF_3-(CF_2^-)_6-CF_2-SO_3H$	6.2757	56.230	months	recalcitrant
$C_6H_5-O-CF_2-CF_2-SO_3H$	2.3298	3.162	days to weeks	weeks to months

[a] Estimated using EPI Suite, environmental fate estimation models developed by the EPA's Office of Pollution Prevention Toxics and Syracuse Research Corporation (SRC).

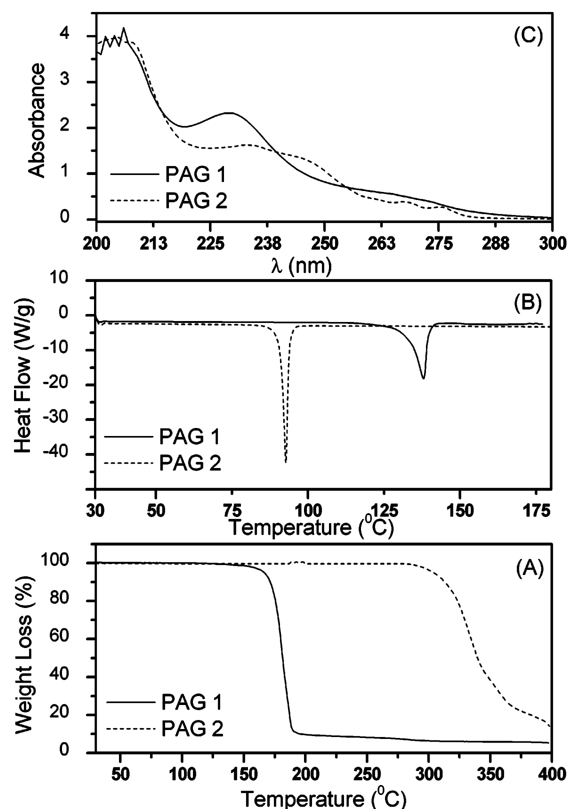

Figure 3. (A and B) Thermal and (C) absorption properties of PAG 1 and 2.

photoacid generators worthwhile. In addition, the sodium salt of aryloxyperfluoroethanesulfonates have been isolated and laboratory experiments are in progress to determine quantitatively the fate of aryloxyperfluoroethanesulfonate in the environment.

3.2.3. Thermal, Temporal, and Photochemical Stability. Photoacid generators require superior thermal and storage stability to avoid acid and other undesirable product formation by non-photochemical pathways.[26,61] In addition, photochemically generated acid and other products should be nonvolatile and stable.[62,63] Lower thermal and storage stability influences the lithographic performance of the resist, whereas the latter affects the lifetime of the exposure tool when it is performed under high vacuum. The thermal stability of PAGs in their neat form was investigated by DSC and TGA (panels A and B of Figure 3). The PAG 1 containing diphenyliodonium cation is stable up to 160 °C. The same PAG anion carrying the sulfonium cation (PAG 2) shows higher stability

(62) Chauhan, M. M.; Nealey, P. F. *J. Vac. Sci. Technol., B* **2000**, *18*, 3402.
(63) Dentinger, P. M. *J. Vac. Sci. Technol., B* **2000**, *18*, 3364.

(>300 °C) and suggests that the stability in onium PAGs can be controlled by choosing the appropriate photosensitive cation. From TGA and DSC data (Table 1), both PFOS-free and PFBS PAGs are stable in neat forms and nonvolatile up to 150 °C.

The storage stability of the PFOS-free PAG both neat and in DUV formulations was studied under ambient conditions. We did not observe any structural changes even after 1 year, as indicated by ^{1}H and ^{19}F NMR analysis, suggesting that the new PAGs are stable in their neat form. PAG decomposition in the formulation alters their lithographic performance, including their resist sensitivity (E_0). A resist solution (P(HS-*co*-S-*co*-tBA), 10% tBA) was exposed to 254 nm radiation 5 days after preparation and its sensitivity was compared to fresh material (see the Supporting Information). The dose to clear (E_0) value increased slightly for all the resists, but the increase is also dependent on the PAG cation. The iodonium PAGs (PAG 1 and DPI PFBS) showed higher variations than sulfonium PAGs (PAG 2 and TPS PFBS), and their performance was consistent with the higher formulation stability observed for sulfonium PAGs in the literature. In addition to the PAG cation, the PAG stability in the formulation also depends on the nature of the polymer used, polymer end groups, solvent, and additives present. Although the new PAG contains PAG anion carrying active functional groups (ether linkage, C═C bond), it still has a considerable amount of structural stability in neat as well as resist formulation.

The quantification of photochemically generated fragments from the new PAGs under EUV radiation is relevant to both e-beam and EUV lithography because they are performed under high vacuum conditions.[4,15,62,63] Thin films of poly-(4-hydroxystyrene-*co*-4-*tert*-butoxycarbonyloxystyrene) containing PAG 1 and PAG 2 were analyzed after being exposed to EUV wavelength radiation. The volatile emission products from thin films that appeared on exposure to EUV radiation at higher than acceptable amounts (1×10^{12} molecules/cm^2) were benzene (2.76×10^{14} molecules/cm^2) and iodobenzene (6.33×10^{13} molecules/cm^2). The main sources for both fragments are expected to be from the photosensitive chromophore, as the onium chromophore undergoes homo- or heterolytic fragmentation under high-energy radiation by either a direct process or a resist-induced process as expected. The extent of emission of volatile products from chemically amplified resist also depends on the composition of the particular photoresist and their preparative methods. The relationship between molecular weight, boiling point, and vapor pressure of various photoproducts and their outgassing characteristics at 157 nm was reported earlier.[64] However, emission of volatile products at EUV wavelengths is an important concern, and it has been shown that changing the resist composition and PAG chromophores can reduce the concentration of volatile of products.[53,63]

3.2.4. Optical Characteristics. PAG absorption is increasingly a critical factor for good lithographic performance at shorter wavelengths.[42,65,66] Strong absorption results in poor resist profiles, whereas low absorption results in poor resist sensitivity. We measured the UV absorption of PAGs in solution (Figure 3C) as well as in a resist formulation (spin coated on a quartz plate) at same molar concentration. The PAGs show strong absorption only below 250 nm. PAG 2 ($\epsilon_{248\ \mathrm{nm}}$ (acetonitrile, M^{-1} cm^{-1}) = 15 887) shows a higher molar absorption coefficient than PAG 1 ($\epsilon_{248\ \mathrm{nm}}$ (acetonitrile, M^{-1} cm^{-1}) = 6015), even though both of the PAGs carry the same anion (Table 1). However, both iodonium (PAG 1 and DPI PFBS) and sulfonium PAGs (PAG 2 and TPS PFBS) show nearly identical absorption coefficients, even though the PAGs carry different anions. In solution at DUV wavelengths, the results indicate that PAG absorption is mainly influenced by the chromophore and that the influence of the anion is small. These results are consistent with the literature reported for onium PAGs.[3,59]

Subsequently, we measured the UV absorption of PAG-containing films (spin coated on quartz plate). PAG absorbance was calculated by subtracting the total absorbance from polymer absorbance as described in the literature.[51] The UV−VIS spectra measured in a PHS film indicates that all the PAGs have acceptable transparency at 254 nm. PAG absorption is $<0.02\ \mu$m^{-1}. However, the absorbance of EUV wavelength radiation of any material is quite different from DUV absorbance and is the sum of the atomic absorption of its constituent atoms. The common PAG elements such as I, F, and O absorb strongly.[42] We calculated the EUV absorbance of PHS resist polymers containing PAGs of 10 wt % as described in the Experimental Section. The EUV absorbance calculated using photoabsorption cross-section and the density of the polymer agrees well with measured EUV absorption.[42] The absorbance characteristics of the PAGs (PAG 1 and DPI PFBS) are comparable at 254 nm ($\leq 0.02\ \mu$m^{-1}), but higher absorption was observed for the standard PAG at EUV wavelength. As a result of reduced fluorine content, the PFOS-free PAGs therefore show better transparency than standard PAGs, as expected (PAG 2 > TPS PFBS; PAG1 > DPI PFBS). The details of the calculations and the plots are provided in the Supporting Information. It has been shown that the combination of both PAG efficiency and transparency affect the resist performance at shorter wavelengths.[41,65,66] Higher transparency at EUV wavelength, with reasonable thermal stability and good solubility of the new PAGs, means increased process flexibility and performance.

3.2.5. Photoacid Generation and Photosensitivity. The most important property of a PAG is its ability to generate acid upon irradiation. This property was confirmed by both IR and UV−VIS spectroscopy. The photoacid generation in solution was detected by employing Rhodamine B (Rb), a xanthene dye whose optical properties change upon protonation.[67] This property was used to detect acid generation by a PAG in nonaqueous media using a UV−VIS spectro-

(64) Houlihan, F. M.; Rushkin, I. L.; Hutton, R. S.; Timko, A. G.; Reichmanis, E.; Nalamasu, O.; Gabor, A. H.; Medina, A. N.; Malik, S.; Neiser, M.; Kunz, R. R.; Downs, D. K. *J. Photopolym. Sci. Technol.* **1999**, *12*, 525.

(65) Cameron, J. F.; Chan, N.; Moore, K.; Pohlers, G. *J. Photopolym. Sci. Technol.* **2001**, *14*, 345.

(66) Cameron, J. F.; Pohlers, G.; Suzuki, Y.; Chan, N. *J. Photopolym. Sci. Technol.* **2002**, *15*, 453.

(67) Ortica, F.; Pohlers, G.; Coenjarts, C.; Bejan, E. V.; Cameron, J. F.; Zampini, A.; Haigh, M.; Scaiano, J. C. *Org. Lett.* **2000**, *2*, 3591.

photometer. A series of PAG solutions with similar concentrations were prepared and irradiated using a broadband UV−VIS source. After irradiation, an aliquot of Rb was directly added to the irradiated sample and the UV−VIS measurement was performed. The final Rb concentration in the sample was 10−20 μM. The irradiated PAG (1 and 2) solutions absorb strongly at 555 nm upon addition of the Rb solution because of protonation of the Rb lactone ring. In addition, visibly colorless PAG solution becomes pink and confirms acid generation. Photoacid generation in a film was confirmed by the formation of PHS from poly(4-*tert*-butoxycarbonyloxystyrene) by IR spectroscopy.[26] The appearance of a hydroxyl absorbance at 3500 cm^{-1} after irradiation of the polymer with PAGs followed by a mild postexposure bake step at 60 °C results in a decrease in the characteristic *tert*-butoxycarbonyl ester band centered at 1756 cm^{-1} and confirms photoacid generation in the film. The experiments above show the effectiveness of the PAG but the results are qualitative in nature. In microlithography studies, the energy to clear (E_0) and energy to size (E_s) are commonly used as a measure of photosensitivity of a particular CAR system.[4] The smaller the required dose, the more sensitive the resist formulation. Photosensitivity measurements were carried out using a positive tone high-activation-energy resist (P(HS-*co*-S-*co*-tBA); 10% tBA) with ∼ 2 wt % PAG with respect to resist (same molar concentration of PAG). The E_0 was found to be 1.36 mJ/cm^2 for both iodonium PAGs (PAG 1 and DPI PFBS) and 1.53 and 1.70 mJ/cm^2 for PAG 2 and TPS PFBS, respectively, indicating that PAG 1 and 2 behave similarly to the standard PAG (Table 1). To determine the E_s, we performed DUV experiments with standard P(HS-*co*-S-*co*-tBA) photoresist (25% tBA). The resist film containing all the PAGs and a standard P(HS-*co*-S-*co*-tBA) polymer (25% tBA) resolved 1 μm to 500 nm feature size upon exposure to 254 nm. The E_s values for all the PAGs were in the range of 8−10 mJ/cm^2. The optical micrographs recorded for a DUV-exposed film containing P(HS-*co*-S-*co*-tBA)/PAG 2 and P(HS-*co*-S-*co*-tBA)/TPS PFBS are available in the Supporting Information. The experiment above confirms that the performance of the new PAGs in chemically amplified resists is comparable to or better than conventional, less environmentally friendly PFOS- and PFAS-based PAGs.

3.3. E-beam and EUV Lithography Imaging. The role of PFOS-free PAGs as an effective tool to catalyze the deprotection of high-activation type acid labile groups (∼35 kcal/mol) in a positive tone chemically amplified resist is best demonstrated through e-beam and EUV lithography. E-beam experiments were performed to understand the basic lithographic response (sensitivity and resolution) of these PAGs, because e-beam patterning is considered to be a close analogue of EUV lithography.[68] The same resist compositions were then evaluated in EUV lithography experiments. High-activation type P(HS-*co*-S-*co*-tBA)[69] and P(GBLMA-*co*-MAdMA)[70] photoresists were selected for imaging experiments, as both are extensively used photoresist materials for 248 and 193 nm lithography with potential for EUV lithography application.[4,18]

The lithographic experiments were conducted using standard processing conditions, including commonly used solvents and developer. The best and most reproducible results in terms of sensitivity and resolution were achieved by optimizing the processing conditions used for DUV lithography. As discussed earlier, initial imaging characteristics of PFOS-free PAGs as well as PFBS PAGs in P(GBLMA-*co*-MAdMA) and P(HS-*co*-S-*co*-tBA) photoresists were evaluated using e-beam radiation. As an example, Figures 4 and 5 show top-down SEM micrographs obtained for a resist film containing P(GBLMA-*co*-MAdMA)-iodonium PAG and P(HS-*co*-S-*co*-tBA)-sulfonium PAG after development with 0.26 N TMAH. P(GBLMA-*co*-MAdMA)-sulfonium PAG and P(HS-*co*-S-*co*-tBA)-iodonium PAG resist performance under e-beam radiation and the high-resolution SEM images are shown in the Supporting Information.

In general, the dose to print sub-100 nm (1:2, 1:1, 1:2 lines/space) lines and spaces (L/S) is lower than 28 μC/cm^2 for all resists. Specifically, the P(HS-*co*-S-*co*-tBA) composition shows high resist sensitivity ($<$18 μC/cm^2) compared to P(GBLMA-*co*-MAdMA) ($<$28 μC/cm^2), but the latter shows higher resolution than the former. The LER for lithographically printed dense 100 nm lines and spaces is less than 10 nm for all resists, but smaller differences were observed between certain polymer/PAG compositions. As demonstrated previously by other researchers, the variation observed here for PAG lithographic performance in P(G-BLMA-*co*-MAdMA) and P(HS-*co*-S-*co*-tBA) photoresists could be due to the difference in processing conditions, resist−PAG combinations, nonresist parameters, or some combination of each. Despite the small variations in lithographic performance, PFOS-free resist systems are promising materials for sub-100 nm patterning applications, as observed from their high sensitivity, resolution, and comparable LER values. In addition, the top-down SEM micrographs shown in Figures 4 and 5 understandably show the performance of new PFOS-free PAGs to those of standard PFBS PAGs and their potential for EUV lithography applications.

Subsequently, EUV lithography experiments were performed with films containing P(GBLMA-*co*-MAdMA) photoresist and PFOS-free as well as PFBS onium PAGs. We selected the P(GBLMA-*co*-MAdMA) photoresist because it shows better overall imaging performance with e-beam radiation under simple processing conditions. Line and space patterns down to 30 nm were resolved. The dose required to resolve sub-40 nm L/S for the all the resists were lower than 8.6 mJ/cm^2. Figure 6 shows high-resolution SEM micrographs of the P(GBLMA-*co*-MAdMA)-sulfonium PAG resist that was exposed to EUV radiation and developed using aqueous 0.26 N TMAH. The SEM images obtained for P(GBLMA-*co*-MAdMA)-iodonium PAG are shown in the Supporting Information.

The versatility of PFOS free PAG for EUV lithography application was further demonstrated by applying them beyond conventional polymeric photosensitive systems. We investigated the EUV lithographic performance of sulfonium

(68) Lingnau, J.; Dammel, R.; Theis, J. *Solid State Technol.* **1989**, *32*, 107.
(69) Ito, H.; Breyta, G.; Hofer, D.; Sooriyakumaran, R.; Petrillo, K.; Seeger, D. *J. Photopolym. Sci. Technol.* **1994**, *7*, 433.
(70) Nozaki, K.; Yano, E. *J. Photopolym. Sci. Technol.* **1997**, *10*, 545.

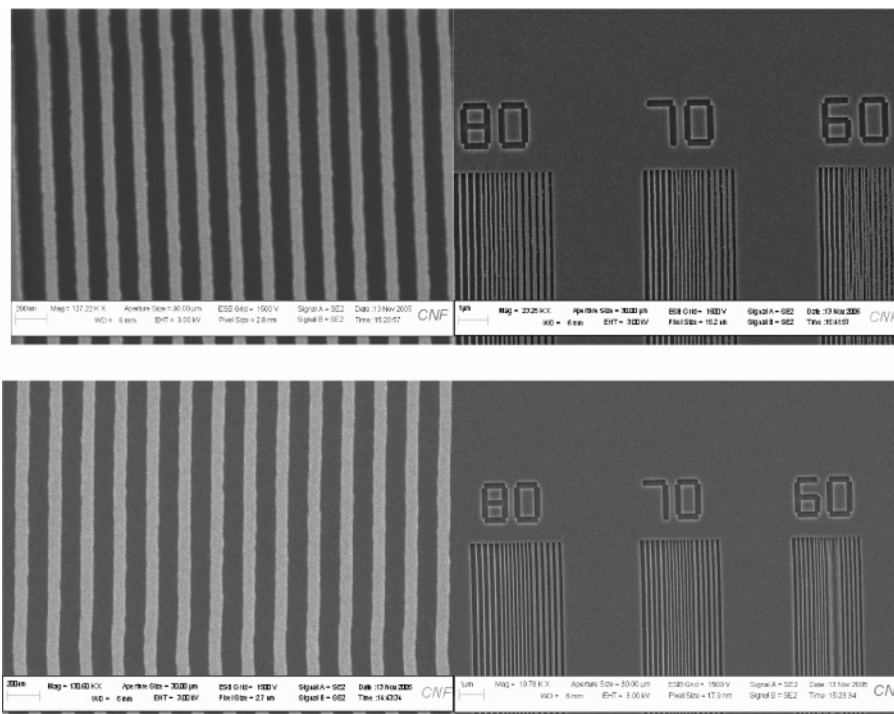

Figure 4. High-resolution line-spaces for e-beam-exposed P(GBLMA-*co*-MAdMA) film containing DPI PFBS (top, $E_s = 16\ \mu C/cm^2$) and PAG 1 (bottom, $E_s = 24\ \mu C/cm^2$). Processing conditions: PAB = 115 °C/60 s; PEB = 120 °C/60 s; development = 0.26 N TMAH/30 s.

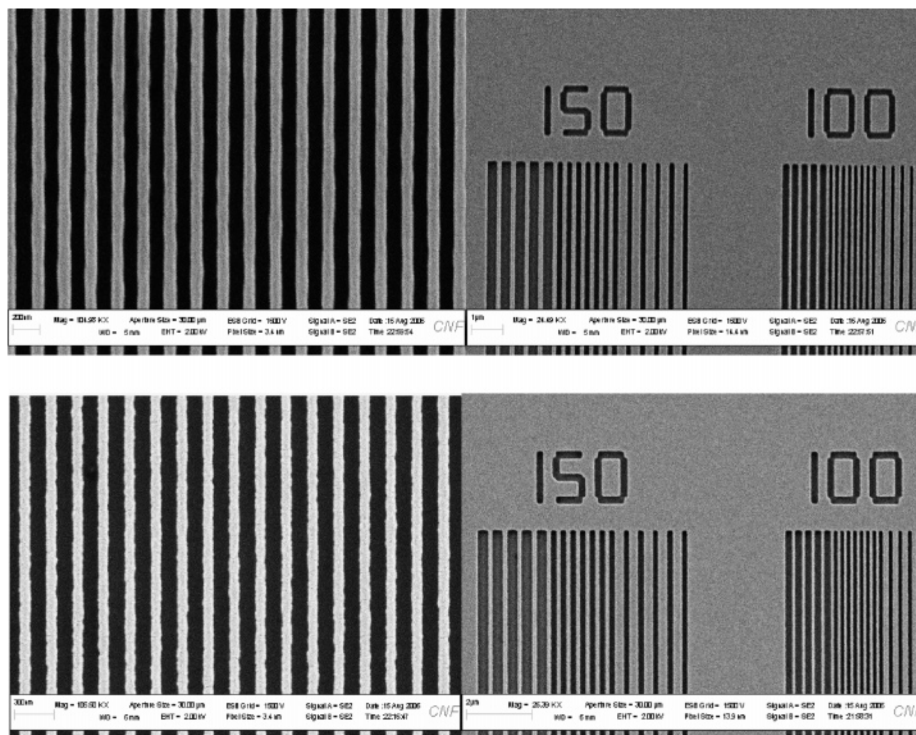

Figure 5. High-resolution line-spaces for e-beam-exposed P(HS-*co*-S-*co*-tBA) resist containing TPS PFBS (top, $E_s = 16\ \mu C/cm^2$) and PAG 2 (bottom;, $E_s = 16\ \mu C/cm^2$). Processing conditions: PAB = 140 °C/60 s; PEB = 130 °C/60 s; development = 0.26 N TMAH/30 s.

PAGs in *tert*-butyloxycarbonyl-protected C-4-hydroxyphenyl calix[4] resorcinarene, a high-resolution molecular glass resist developed in our group for EUV lithography applications.[50] The PAG 2−molecular glass resists ($E_s = 21$ mJ/cm^2; $R =$ 30−25 nm) performance is comparable to that of TPS PFBS ($E_s = 39$ mJ/cm^2; $R = 35-30$ nm) performance as observed with polymeric resist.[50,71] The line-edge roughness for dense 60 nm lines and spaces for both the resists is approximately 5 nm and is comparable within the estimation error.[71] It is clear from the EUV experiments that patterning down to 30 nm can be readily accomplished for formulations containing the PFOS-free PAGs and both conventional and unconventional photoresists. These preliminary findings suggest that it may be possible to further increase the lithographic performance of the PFOS-free systems through optimization

(71) Ayothi, R.; Chang, S. W.; Felix, N.; Cao, H. B.; Deng, H.; Wang, Y.; Ober, C. K. *J. Photopolym. Sci. Technol.* **2006**, *19*, 515.

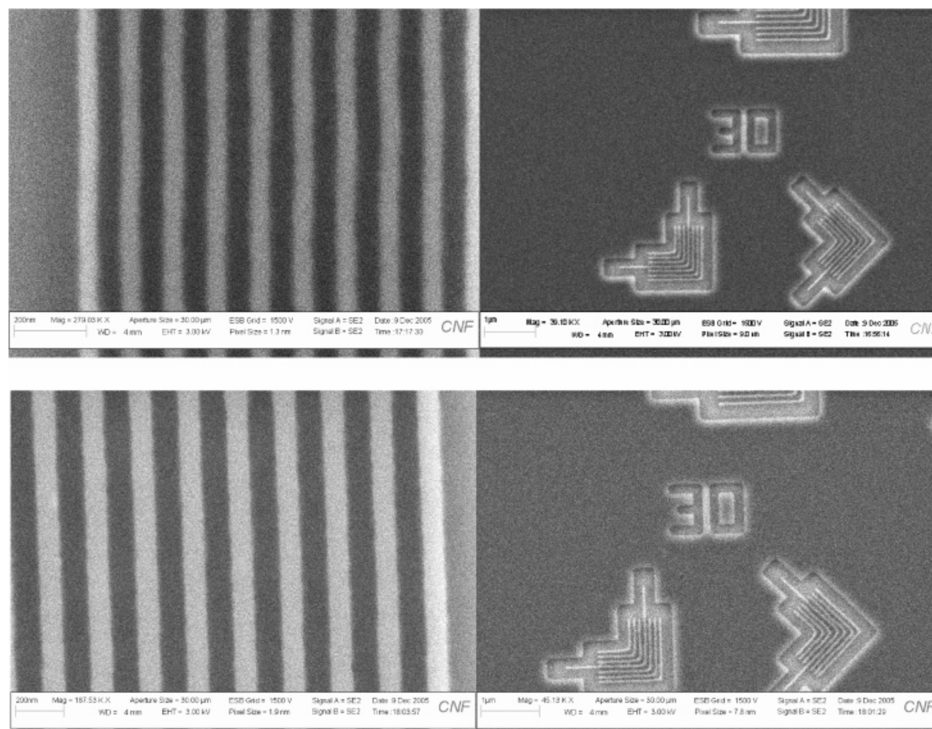

Figure 6. SEM micrographs obtained with P(GBLMA-*co*-MAdMA) film containing TPS PFBS (top, E_s = 8.6 mJ/cm^2; LER (100 nm 1:1 L/S) = 8.6 ± 0.6 nm) and PAG 2 (bottom; E_s = 7.5 mJ/cm^2; LER (100 nm 1:1 L/S) = 7.7 ± 0.8 nm) exposed to EUV radiation and developed using 0.26 N TMAH.

of various resist parameters, as demonstrated previously by other researchers for various resist systems. The results shown above undoubtedly confirm that the new PFOS-free PAGs with reduced fluorine content do generate strong acid and can resolve image profiles similar to those of standard PFBS PAGs as well as show their potential for EUV lithography application.

4. Conclusions

We have developed the first examples of PFOS-free ionic PAGs composed of diphenyliodonium and triphenylsulfonium cations with the environmentally compatible 2-phenoxytetrafluoroethanesulfonate anion. Evaluation of lithographically relevant properties such as solubility, thermal stability, absorption, and acid generation capabilities of the new PAGs shows they have properties comparable to those of PFOS-based PAGs. Lithographic performance of the PAGs was tested with model photoresists using both e-beam and EUV radiation and shows high sensitivity, resolution, and acceptable line edge deviations to those of standard PAGs under simple nonoptimized processing conditions. Comparison of properties and lithographic performance of the new reduced fluorine PAGs in model photoresists demonstrates their performance similarity to existing PFAS PAGs and their potential for lithography applications such as EUV lithography.

Acknowledgment. This work was supported by the Intel Corporation. This work utilized in part the facilities provided by the Cornell Nanoscale Science and Technology Facility (CNF) and the Cornell Center for Materials Research (CCMR). The LER program was provided by Patrick Naulleau's research group, CNSE at University of Albany. The authors thank Brian Hoef and Paul Denham for help with EUV exposures.

Supporting Information Available: (i) Details about the estimation of bioaccumulation related properties; (ii) NMR spectra of PAGs and their intermediates; (iii) GC/MS spectra of the liquid compound; (iv) ESI/MS spectra of PAGs; (v) experimental transmittance spectrum of PAGs in PHS film; (vi) calculated EUV transmittance spectra of PAGs in PHS film; (vii) UV−VIS and FT−IR spectra of the detection of photoacid generation in solution and film; (viii) optical micrographs of DUV imaging and formulation stability study at DUV; (ix) summary of outgassing fragments from PAG at EUV; and (x) SEM micrographs and details about lithographic performance at e-beam and EUV. This material is available free of charge via the Internet at http://pubs.acs.org.

CM062802K